

Dynamics of Cavitating Pumps

Another very different example of the importance of kinematic waves and their interaction with dynamic waves occurs in the context of cavitating pumps. The dynamics of cavitating pumps are particularly important because of the dangers associated with the instabilities such as cavitation surge (see section (Nri)) that can result in very large pressure and flow rate oscillations in the entire system of which the pumps are a part (Brennen 1994). Therefore, in many pumping systems (for example the fuel and oxidizer systems of a liquid-propelled rocket engine), it is very important to be able to evaluate the stability of that system and knowledge of the transfer function for the cavitating pumps is critical to that analysis (Rubin 1966).

For simplicity in this analytical model, the pump inlet and discharge flows are assumed to be purely incompressible liquid (density ρ_L). Then the inlet and discharge flows can be characterized by two flow variables; convenient choices are the total pressure, p_i^T , and the mass flow rate, \dot{m}_i , where the inlet and discharge quantities are given by $i = 1$ and $i = 2$ respectively as described in section (Nrl). Consider now the form of the transfer function (equation (Nrl6)) connecting these fluctuating quantities. As described in section (Nrl) the transfer function will be a function not only of frequency but also of the pump geometry and the parameters defining the mean flow (see section (Nkh)). The instantaneous flow rates at inlet and discharge will be different because of the rate of change of the total volume, V , of cavitation within the pump. In the absence of cavitation, the pump transfer function is greatly simplified since (a) if the liquid and structural compressibilities are neglected then $\dot{m}_1 = \dot{m}_2$ and it follows that $T_{21} = 0$, $T_{22} = 1$ and (b) since the total pressure difference across the pump must be independent of the pressure level it follows that $T_{11} = 1$. Thus the non-cavitating transfer function has only one non-trivial component, namely T_{12} where $-T_{12}$ is known as the pump impedance. As long as the real part of $-T_{12}$, the pump resistance, is positive, the pump is stable at all frequencies. Instabilities only occur at off-design operating points where the resistance becomes negative (when the slope of the total pressure rise against flow rate characteristic becomes positive). Measurements of T_{12} (which is a function of frequency) can be found in Anderson *et al.* (1971) and Ng and Brennen (1976).

A cavitating pump is much more complex because all four elements of $[T]$ are then non-trivial. The first complete measurements of $[T]$ were obtained by Ng and Brennen (1976) (see also Brennen *et al.* 1982). These revealed that cavitation could cause the pump dynamic characteristics to become capable of initiating instability in the system in which it operates. This helped explain the cavitation surge instability described in section (Nri). Recall that cavitation surge occurs when the pump resistance (the real part of $-T_{12}$) is positive; thus it results from changes in the other elements of $[T]$ that come about as a result of cavitation.

A quasistatic approach to the construction of the transfer function of a cavitating pump was first laid out by Brennen and Acosta (1973, 1976) and proceeds as follows. The steady state total pressure rise across the pump, $\Delta p^T(p_1^T, \dot{m})$ and the steady state volume of cavitation in the pump, $V(p_1^T, \dot{m})$ will both be functions of the mean mass flow rate \dot{m} . They will also be functions of the inlet pressure (or, more accurately, the inlet pressure minus the vapor pressure) because this will change the cavitation number and the total pressure rise may depend on the cavitation number as discussed in section (Nkh). Note that V is not just a function of cavitation number but also depends on \dot{m} because changing \dot{m} changes the angle of incidence on the blades and therefore the volume of cavitation bubbles produced. Given these two

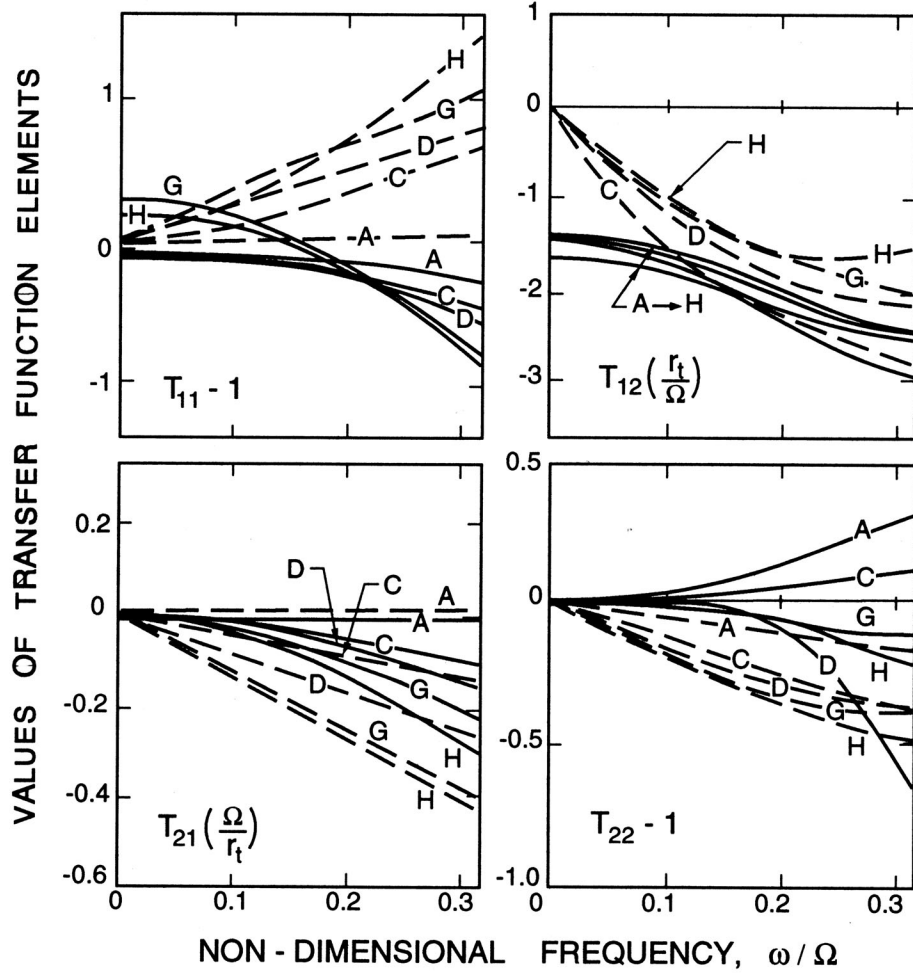


Figure 1: Typical measured transfer functions for a cavitating pump operating at five different cavitation numbers, $\sigma =$ (A) 0.37, (C) 0.10, (D) 0.069, (G) 0.052 and (H) 0.044. Real and imaginary parts which are denoted by the solid and dashed lines respectively, are plotted against the non-dimensional frequency, ω/Ω ; r_t is the impeller tip radius. Adapted from Brennen *et al.* (1982).

functions we could then construct the quasistatic or low frequency form of the transfer function as

$$[T] = \begin{bmatrix} 1 + \frac{d(\Delta p_1^T)}{dp_1^T} \Big|_{\dot{m}} & \frac{d\Delta p_1^T}{d\dot{m}} \Big|_{p_1^T} \\ i\omega\rho_L \frac{dV}{dp_1^T} \Big|_{\dot{m}} & 1 + i\omega\rho_L \frac{dV}{d\dot{m}} \Big|_{p_1^T} \end{bmatrix} \quad (\text{Nsi1})$$

The constant $K^* = -\rho_L(dV/dp_1^T)_{\dot{m}}$ is known as the *cavitation compliance* while the constant $M^* = -\rho_L(dV/d\dot{m})_{p_1^T}$ is called the *cavitation mass flow gain factor*. Later, we comment further on these important elements of the transfer function.

Typical measured transfer functions (in non-dimensional form) for a cavitating pump are shown in figure 1 for operation at four different cavitation numbers. Note that case (A) involved virtually no cavitation and that the volume of cavitation increases as σ decreases. In the figure, the real and imaginary parts of each of the elements are shown by the solid and dashed lines respectively, and are plotted against a non-dimensional frequency. Note that both the compliance, K^* , and the mass flow gain factor, M^* , increase monotonically as the cavitation number decreases.

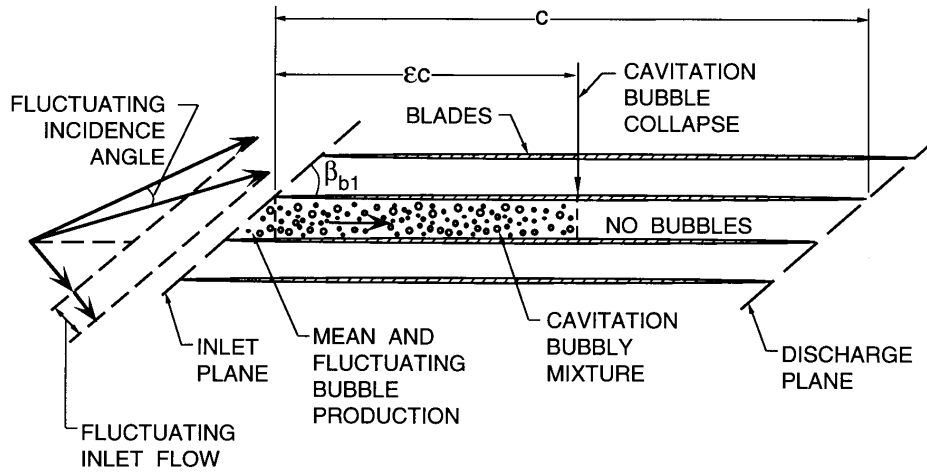


Figure 2: Schematic of the bubbly flow model for the dynamics of cavitating pumps (adapted from Brennen 1978).

In order to model the dynamics of the cavitation and generate some understanding of data such as that of figure 1, we have generated a simple bubbly flow model (Brennen 1978) of the cavitating flow in the blade passages of the pump. The essence of this model is depicted schematically in figure 2, that shows the blade passages as they appear in a developed, cylindrical surface within an axial-flow impeller. The cavitation is modeled as a bubbly mixture that extends over a fraction, ϵ , of the length of each blade passage before collapsing at a point where the pressure has risen to a value that causes collapse. This quantity, ϵ , will in practice vary inversely with the cavitation number, σ , (experimental observations of the pump of figure 1 indicate $\epsilon \approx 0.02/\sigma$) and therefore ϵ is used in the model as a surrogate for σ . The bubbly flow model then seeks to understand how this flow will respond to small, linear fluctuations in the pressures and mass flow rates at the pump inlet and discharge. Pressure perturbations at inlet will cause pressure waves to travel through the bubbly mixture and this part of the process is modeled using a mixture compressibility parameter, K^{**} , that essentially fixes the wave speed. In addition, fluctuations in the inlet flow rate produce fluctuations in the angle of incidence that cause fluctuations in the rate of production of cavitation at inlet. These disturbances would then propagate down the blade passage as kinematic or concentration waves that travel at the mean mixture velocity. This process is modeled by a factor of proportionality, M^{**} , that relates the fluctuation in the angle of incidence to the fluctuations in the void fraction. Neither of the parameters, K^{**} or M^{**} , can be readily estimated analytically; they are, however, the two key features in the bubbly flow model. Moreover they respectively determine the cavitation compliance and the mass flow gain factor; see Brennen (1994) for the specific relationships between K^{**} and K^* and between M^{**} and M^* . Comparison of the model predictions with the experimental measurements indicate that $K^{**} = 1.3$ and $M^{**} = 0.8$ are appropriate values and, with these, the complete theoretical transfer functions for various cavitation numbers are as depicted in figure 3. This should be compared with the experimentally obtained transfer functions of figure 1. Note that, with only a small number of discrepancies, the general features of the experimental transfer functions, and their variation with cavitation number, are reproduced by the model.

Following its verification, we must then ask how this knowledge of the pump transfer function might be used to understand cavitation-induced instabilities. In a given system, a stability analysis requires a complete model (transfer functions) of all the system elements; then a dynamic model must be constructed for the entire system. By interrogating the model, it is then possible to identify the key physical processes that promote instability. In the present case, such an interrogation leads to the conclusion that it is the formation and propagation of the kinematic waves that are responsible for those features of the transfer function (in particular the mass flow gain factor) that lead to cavitation-induced instability. In comparison,

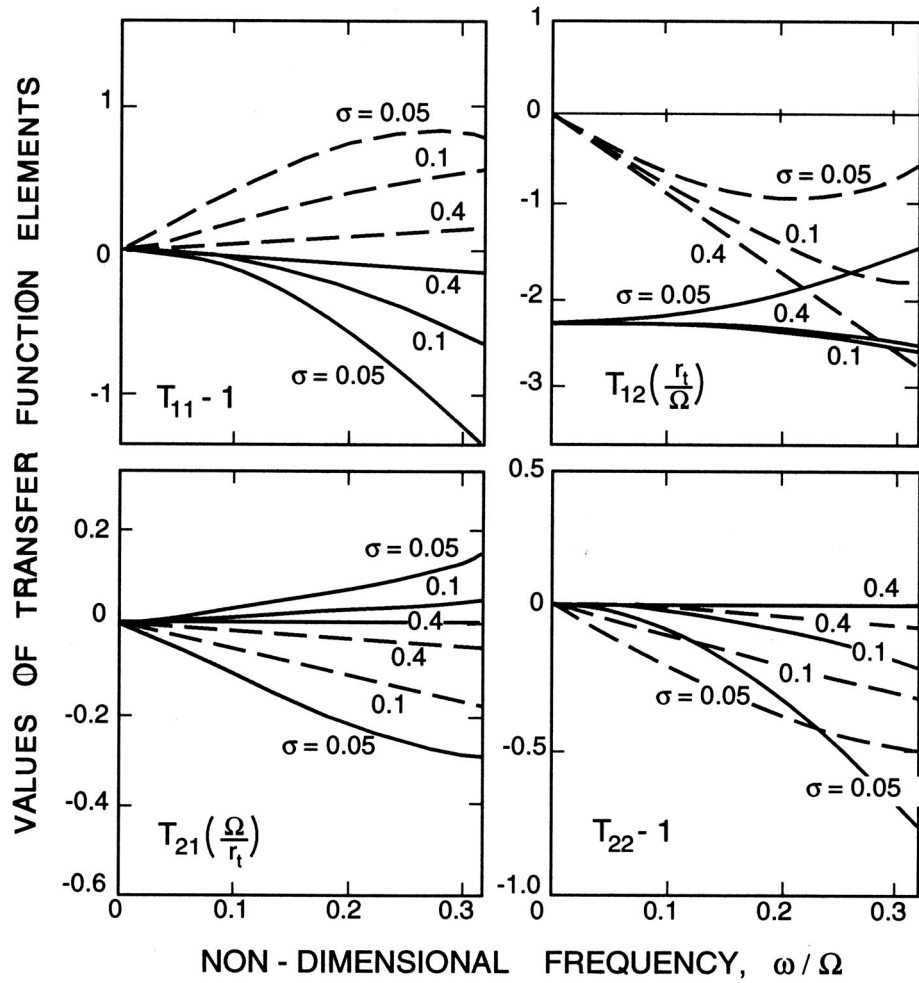


Figure 3: Theoretical transfer functions calculated from the bubbly flow model for comparison with the experimental results of figure 1. The calculations use $K^{**} = 1.3$ and $M^{**} = 0.8$ (adapted from Brennen *et al.* 1982).

the acoustic waves and the cavitation compliance have relatively benign consequences. Hence a more complete understanding of the mass flow gain factor and the kinematic wave production processes that contribute to it will be needed to enhance our ability to predict these instabilities.